RSC Advances

ROYAL SOCIETY OF CHEMISTRY

www.rsc.org/advances

RSC Advances

RSCPublishing

PAPER

Graphic Abstract

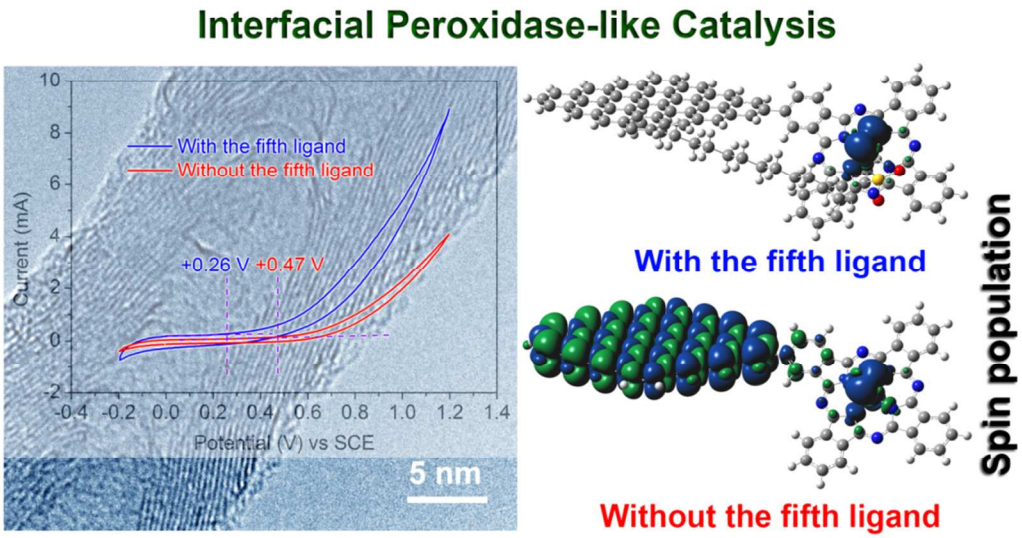

RSC Advances

RSCPublishing

PAPER

Interfacial peroxidase-like catalytic activity of surface-immobilized cobalt phthalocyanine on multiwall carbon nanotubes

Cite this: DOI: 10.1039/xoxxooooox

Received ooth January 2012,
Accepted ooth January 2012

DOI: 10.1039/xoxxooooox

www.rsc.org/

Nan Li,[a] Wangyang Lu,*[a] Kemei Pei,[b] and Wenxing Chen*[a]

Rapid diffusional mass transfer process (DMTP) always results in a highly efficient reaction. Here, cobalt phthalocyanine (CoPc) was covalently anchored on multiwall carbon nanotubes (MWCNTs) by an easy and moderate one-step deamination method to obtain the catalyst, MWCNT-immobilized CoPc (CoPc-MWCNTs). The interfacial peroxidase-like catalytic activity of CoPc-MWCNTs has been described for controllable H_2O_2 activation. According to the experimental results and density functional theory calculations, it can be confident that the high-valent cobalt-oxo intermediates are formed during the H_2O_2 activation. Such active species are anchored and exposed on the surface of MWCNTs, shortening the DMTP and enhancing the resistance of CoPc-MWCNTs to oxidative decay. The introduction of linear alkylbenzene sulfonates (LAS) facilitate the catalytic H_2O_2 activation by CoPc-MWCNTs, meanwhile, CoPc-MWCNTs could maintain a high and sustained catalytic activity because of the specific hydrophobic interactions between the long-chain alkyl group of LAS and the π-conjugated surface of MWCNTs.

1 Introduction

Hydrogen peroxide (H_2O_2) is an environmentally friendly oxidant used for organic synthesis, bleaching processes in paper and textile industries, wastewater treatment and for various disinfection applications.[1-3] Recently, much attention has been devoted to the selective activation of H_2O_2 by the catalytic systems based on coordination complex catalysts.[4,5] Strategies to develop these catalysts for oxidation reactions are focused on the introduction of supports to improve their performance and stability.[6,7] Typically, the introduction of the supports does not change the reaction mechanism in essence, however, a major challenge lies in precisely controllable H_2O_2 activation to generate the requisite active intermediates (such as hydroxyl radicals (•OH) and metal-based oxidants), which determines the activity and durability of the complex catalysts, even the utilization of H_2O_2.[8-10] In contrast to synthetic catalysts, enzymes are able to achieve excellent selectivity through specific interaction between substrate and protein environment around the active sites or cofactors.[11] In some metalloporphyrin-based enzymatic reaction systems, the reaction channels are determined by the fifth ligands. For example, horseradish peroxidase and catalase present the corresponding peroxidase-like and catalase-like activities in the presence of the imidazole ligand and phenolate ligand respectively.[12,13] In addition, the protein backbone of enzymes also plays a role in protecting the active sites and isolating them from each other to avoid their self-oxidation.

Recently, the controllable H_2O_2 activation has been achieved by employing the cellulose matrix to mimic the protein backbone of enzymes, and the reaction channel of H_2O_2 activation has been changed from hemolytic cleavage of peroxide O-O bond with the generation of •OH into heterolytic cleavage without radical production in the presence of the fifth ligands.[14] However, during the common enzymatic reactions, one of the most important steps is the diffusional mass transfer process (DMTP) that substrates and products must transfer across a boundary to get to active sites. Therefore, the catalytic efficiency could be enhanced by shortening the course of DMTP, and the active sites should be in the regions where substrates can easily access into and react with the generated active species. For artificial enzyme-like catalysts, so long as the generated active species are anchored without free movement to attack each other, the active sites could be anchored on the surface of catalysts to shorten the DMTP.

Carbon nanotubes (CNTs) have received an increasing scientific interest because of their unusual conjugated structure, high chemical stability and electrical conductivity, and have been extensively employed for the immobilization of enzymes and catalysts.[15-17] In our previous studies, it has been confirmed that the presence of multiwall carbon nanotubes (MWCNTs) could greatly enhance the catalytic activity of cobalt phthalocyanine (CoPc, an enzyme mimic catalyst) for H_2O_2 activation because of their excellent electrical properties.[18,19] But, with the activity for substrate oxidation (corresponding to the peroxidase-like activity) enhancing, the disproportionation of H_2O_2 also presents an increasing trend by undergoing the decomposition of H_2O_2 to form water and oxygen (corresponding to the catalase-like activity). Typically, the catalase-like process and peroxidase-like process are in competition during the activation of H_2O_2.[20] How to precisely control the reactive channel of H_2O_2 activation towards the peroxidase-like process remains a challenge for the artificial enzyme-like catalysts.

Here, we report a bioinspired catalytic system based on multiwall carbon nanotube-bonded cobalt phthalocyanine (CoPc-MWCNTs), which were prepared by a moderate one-step deamination method, minimizing the damage of the conjugated structure of MWCNTs. Linear alkylbenzene sulfonate (LAS, one of the most widespread surfactants in industrial and domestic wastewater) has been employed as the fifth ligand to axially coordinate with the central cobalt ion of CoPc and help cleave the O-O bond of H_2O_2 heterolytically to achieve the peroxidase-like process. The roles of LAS in the catalytic performance of CoPc-MWCNTs for H_2O_2 activation has been investigated in detail. The possible intermediates generated during the catalytic activation of H_2O_2 have been studied by the electron paramagnetic resonance (EPR) spin-trap technique, electrochemistry method and the density functional theory (DFT) calculations. Our results demonstrate the feasibility of anchoring the active sites on the surface of MWCNTs, and LAS not only manifests the role of the fifth ligand, but also has a great contribution to prevent the agglomeration of catalyst.

2 Experimental

2.1 Materials

MWCNTs (lot no. 035NF) and CoPc were supplied by Tokyo Chemical Industry Co., Ltd. Cobalt tetraaminophthalocyanine (CoTAPc) was laboratory-made.[18] The isoamyl nitrite was purchased from Aladdin Industrial Inc. C.I. Acid Red 1 (AR1, Fig. S1), and sodium 4-ethylbenzenesulfonate (C_2-LAS) was purchased from Acros and was used without further purification. Sodium linear-dodecylbenzenesulfonate (C_{12}-LAS) was obtained from Tianjin Kemiou Chemical Reagent Co., Ltd. The spin trap reagent 5,5-dimethyl-pyrroline-oxide (DMPO) was obtained from Tokyo Kasei Kogyo Co., Ltd. Other reagents were of analytical grade and used without further purification.

2.2 Catalyst preparation

MWCNTs (1.0 g) were dispersed in the DMSO solution with vigorous stirring at 85 °C. Then the DMSO solution of CoTAPc (0.05 g) and isoamyl nitrite were dropped into successively. This reaction was stirred and kept at 85 °C for 12 h. The cooled reaction solution was centrifuged and washed with DMF and ultrapure water, and the centrifugation–wash process was repeated several times to remove ungrafted phthalocyanines. After the deamination reaction between CoTAPc and MWCNTs, the CoPc-MWCNTs were obtained after drying under vacuum. This method has been inspired by the reference 21, and the detailed synthesis was shown in Fig. S2.

2.3 Catalytic activity experiment

AR1 has been employed as a model to investigate the catalytic activity of CoPc-MWCNTs for H_2O_2 activation, and the concentration changes of AR1 are proportional to its absorbance in the UV-vis spectrum. CoPc-MWCNTs (0.2 g/L) in aqueous solution experienced ultrasonic dispersion 30 min in advance, and H_2O_2 (0.01M) was added lastly to start the reaction. The repeated catalytic oxidation was operated ten times, in which the known concentration of AR1 and H_2O_2 has been added to ensure the same initial concentration of substrate and oxidant.

2.4 Analysis

The bonding configurations were investigated using X-ray photoelectron spectroscopy (XPS) on a Thermo Scientific K-Alpha spectrometer (monochromatic Al Kα, 1486.6 eV). Co K-edge X-ray Absorption Near Edge Structure (XANES) spectra and extended X-ray adsorption fine structure (EXAFS) spectra were obtained on the BL14W1 beamline at the Shanghai Synchrotron Radiation Facility (SSRF). The storage ring was operated at 3.5 GeV and 241.6 mA. A Si (1 1 1) double-crystal monochromator was used to minimize the harmonics. The spectra were collected at room temperature in the transmission mode with an energy resolution of 0.3 eV. The transmission electron microscopy (TEM) images were obtained on a JEOL JEM-2100 microscope. The cobalt content in CoPc-MWCNTs was measured using microwave-assisted digestion-flame atomic absorption spectrometry (Thermo Sollar M6), and the calculated content of CoPc in CoPc-MWCNTs is 44.4×10^{-6} mol/g. The UV-vis absorption spectra were obtained on a Hitachi U-3010 spectrophotometer. Cyclic voltammograms (CV) were recorded on an IM6ex (Zahner, Germany) electrochemical workstation using saturated calomel electrode (SCE) as reference electrode, and a Pt wire was employed as a counter electrode. The catalyst powders were dispersed in Nafion solution and sonicated for 60 min. Then the working electrode was prepared by dropping the catalyst solutions onto the carbon fiber paper. Cyclic voltammetry was performed in LAS and Na_2SO_4 solutions (pH 7.55, 0.01 mol/L) at room temperature with a scanning rate of 100 mV/s, and the solutions were flushed with dry nitrogen to remove oxygen from the solutions before the electrochemical experiments. DMPO was employed as the spin-trapper for the radicals in EPR experiments on a Bruker A300 spectrometer, which was used to record the EPR signals of DMPO with settings as follows: center field, 3518 G; sweep width, 80 G; microwave frequency, 9.88 GHz; modulation frequency, 100 kHz; power, 20mW.

3 Results and discussion

3.1 Characterization

A deamination reaction has been used to prepare the catalyst of CoPc-MWCNTs. The TEM images (Fig. 1) showed the obvious change on the wall of MWCNTs after the deamination reaction, indicating that CoPc has been anchored on the surface of MWCNTs. XPS and XANES analysis were performed to probe the bonding configuration of CoPc-MWCNTs. As shown in Fig. 2, the Co 2p and N1s peaks of CoTAPc have been observed in the spectrum of CoPc-MWCNTs, which have not been contained in MWCNTs, suggesting that CoPc was anchored on MWCNTs. From the high resolution Co 2p spectra shown in Fig. S3, it can be seen that the peaks occurred at 795.3 and 779.8 eV are assigned to Co $2p_{1/2}$ and Co $2p_{3/2}$ in the spectrum of CoTAPc, and they cannot be found in MWCNTs. When CoTAPc has been anchored on MWCNTs by the deamination reaction, the peaks of Co $2p_{1/2}$ and Co $2p_{3/2}$ increased to 796.4 and 780.7 eV, respectively. This is due to the removal of electron-donating amino groups (which has been evidenced by the disappeared N 1s peak of amino groups in CoPc-MWCNTs shown in Fig. S4), leading to the declined electron density on the CoPc ring. Thus the electron shield to the inner electrons of the central Co will be weakened, increasing the electron binding energy between Co $2p_{1/2}$ and Co $2p_{3/2}$. For the same reasons, N 1s peaks corresponding to aza-bridging and pyrrole nitrogen atoms increased from 398.1 eV in CoTAPc to 398.9 eV in CoPc-MWCNTs. As can be seen from the results of UV-

vis spectra (Fig. S5), the blue-shift (from 725 to 680 nm) of the characteristic Q-band of CoTAPc in the presence of isoamyl nitrite confirms clearly that the deamination process has been achieved. The obvious CoPc absorption at 680 nm has been observed in the spectrum of CoPc-MWCNTs. Moreover, there is nearly no difference of C1s peak in MWCNTs and CoPc-MWCNTs (the inset of Fig. 2), which indicated that the surface structure of MWCNTs has not been destroyed. Accordingly, we can conclude that CoPc has been anchored on MWCNTs by removing the amino substituents on the CoTAPc. Importantly, such direct bonding between CoPc and MWCNTs can bring a minimal damage to the conjugated structure of MWCNTs. And the results of TGA experiment (Fig. S6) indicate that the direct bonding between CoPc and MWCNTs enhances the stability both of them indeed.

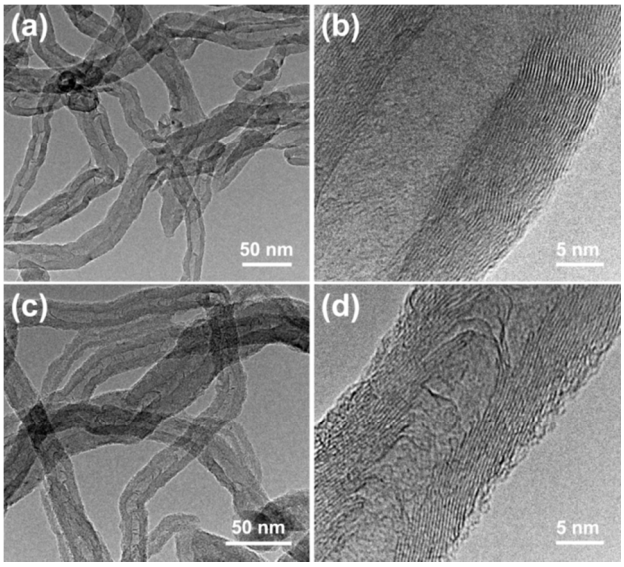

Fig. 1. TEM images of MWCNTs (a, b) and CoPc-MWCNTs (c, d).

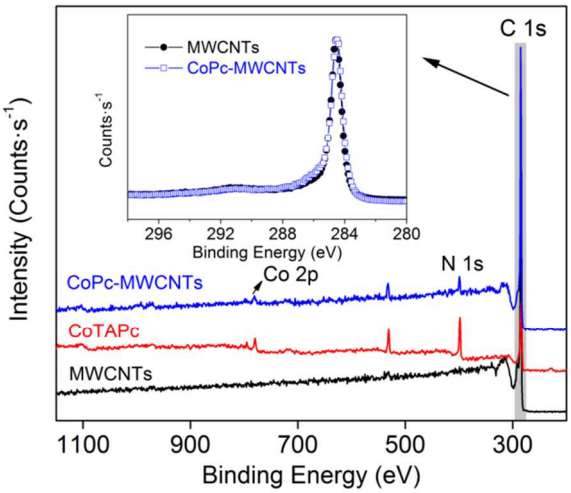

Fig. 2. XPS spectra of MWCNTs, CoTAPc and CoPc-MWCNTs.

To understand the electronic structure of Co ion in catalysts, XANES characterization has been performed. In Figure 3a, the first and second peaks were respectively assigned to a dipole forbidden 1s→3d transition and a shakedown satellite 1s→4p_z transition, and the 1s→4p_z transition is a fingerprint of Co-N_4 structure.[22] A clear decline of 1s→4p_z transition is observed for CoPc-MWCNTs in comparison with CoPc and CoTAPc, indicating π-electron conjugation of CoPc macrocycles has been changed by covalently bonding to MWCNTs, which would a strong influence on the coordination between Co ions and other ligands including the H_2O_2. It can also be seen in the EXAFS spectra (Fig. 3b) that the atomic distance R between the Co ion and the nearest neighbor N has a slight decrease, resulting in a change in the coordination environment of central cobalt ion. In addition, the 1s→3d transition shown in the XANES spectra of CoPc-MWCNTs may be because that the symmetrical structure of CoPc changes into inversion symmetry after being covalently bonded with MWCNTs. And such results could not be observed in the spectra of mixture of CoPc and MWCNTs.[23]

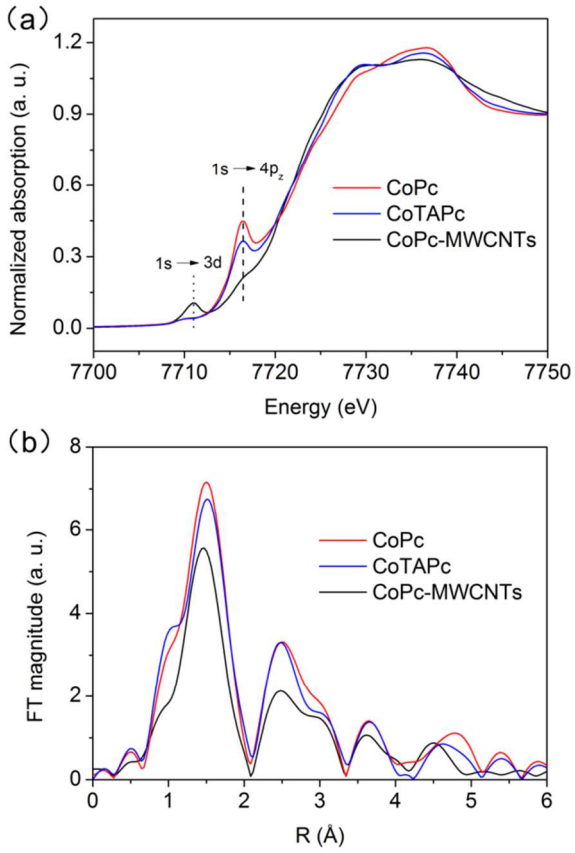

Fig. 3. XANES (a) and EXAFS (b) spectra of CoPc, CoTAPc and CoPc-MWCNTs.

3.2 Catalytic Activity for H_2O_2 activation

AR1 has been employed as a model to investigate the catalytic activity of CoPc-MWCNTs for H_2O_2 activation. Fig. 4 shows that CoPc-MWCNTs exhibited a high catalytic activity for activating H_2O_2 to oxidize AR1 in the presence of C_{12}-LAS, while such high activity for H_2O_2 activation has not been observed in the system of CoPc-MWCNTs without C_{12}-LAS or the system of C_{12}-LAS without CoPc-MWCNTs. Although a high catalytic activity for H_2O_2 activation had been presented in the previous CoTAPc-MWCNTs system without LAS, the high-concentration H_2O_2 (0.1 M) was essential to maintain throughout the reaction due to the competition between catalase-like and peroxidase-like process, and most of H_2O_2 has been consumed by decomposing into water and oxygen.[18] However, in the presence of C_{12}-LAS, CoPc-MWCNTs exhibit a high activity even with low-concentration H_2O_2 (0.01 M), indicating that a different reaction channel of H_2O_2 activation has been achieved towards the peroxidase-like process. Compared with the

catalytic system based on cellulose fiber bonded CoTAPc,[14] an enhanced activity has been achieved under the same conditions by anchoring the CoPc on the surface of MWCNTs because of the shorten course of DMTP. Moreover, CoPc-MWCNTs still exhibit high catalytic activity for H_2O_2 activation in the presence of C_{12}-LAS every run during the successive oxidation of AR1 (Fig. 5), together with the high catalytic performance at different temperature (Fig. S7), suggesting that CoPc-MWCNTs perform the sufficient stability and are resistant to oxidative decay during the H_2O_2 activation. Accordingly, we could believe that the generated active intermediates might be protected or isolated from each other to minimize the oxidation possibility of active sites.

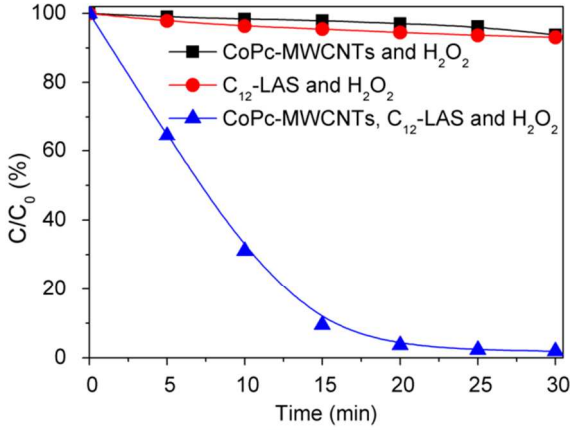

Fig. 4. Concentration changes of AR1 (5×10^{-5}M) under different conditions. ([CoPc-MWCNTs]=0.2 g/L (containing 8.88×10^{-6} M of CoPc), [C_{12}-LAS]=5×10^{-3} M, [H_2O_2]=0.01 M, pH 7.55, 50 °C.)

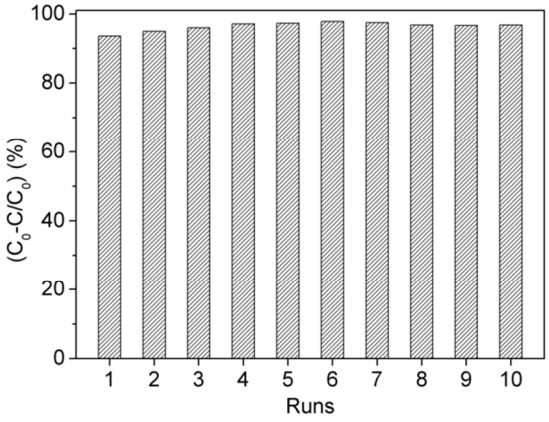

Fig. 5. The cyclic oxidation of AR1 (5×10^{-5} M). ([CoPc-MWCNTs]=0.2 g/L (containing 8.88×10^{-6} M of CoPc), [C_{12}-LAS]=5×10^{-3} M , [H_2O_2]=0.01 M, pH 7.55, 50 °C.)

To further investigate the role of the fifth ligand of LAS in H_2O_2 activation catalyzed by CoPc-MWCNTs, the catalytic oxidations were carried out under the same conditions in the presence of C_2-LAS. As shown in Fig. 6, the catalytic activity of CoPc-MWCNTs for H_2O_2 activation has been enhanced in the presence of C_2-LAS, and such enhanced activity depends on the number of C atoms in alkyl group of LAS, suggesting that the hydrophobic chains of LAS play a noticeable role in this catalytic system. It is generally known that the agglomeration or π-π stacking of CNTs owing to the strong van der Waals forces limits their full utilization, and CNTs could be linearly wrapped along the nanotube by the compounds with chain-like and conjugated structures to improve their dispersion.[24-26] Thus, with the linear long-chain and benzene ring structure, C_{12}-LAS performs the better ability for the dispersion of CoPc-MWCNTs, resulting in the higher activity of CoPc-MWCNTs compared to the short-chain C_2-LAS system. But, the dispersion improvement of CoPc-MWCNTs is part of the reason for the activity enhancement, because the catalytic activity of CoPc-MWCNTs has also been improved in the presence of C_2-LAS which cannot improve the dispersion of CoPc-MWCNTs. The cyclic voltammetry (CV) experiments have been employed to investigate the role of C_{12}-LAS during the H_2O_2 activation catalyzed by CoPc-MWCNTs, in which the electrolytes were C_{12}-LAS and Na_2SO_4 respectively. For the electrochemical oxidation of H_2O_2 catalyzed by CoPc, the possible mechanism is as follows: [27,28]

$$Co^{II}Pc \rightarrow Co^{III}Pc + e^-$$

$$Co^{III}Pc + 1/2\ H_2O_2 \rightarrow Co^{II}Pc + 1/2O_2 + H^+$$

It can be seen from Fig. 7 that the electrocatalytic oxidation of H_2O_2 starts from 0.26 V (in 0.01 M C_{12}-LAS solution) and 0.47 V (in 0.01 M Na_2SO_4 solution). The more negative oxidation potential shown in Fig. 7 indicates that C_{12}-LAS promotes the oxidation of H_2O_2 catalyzed by CoPc-MWCNTs. This enhancement in oxidation peak of H_2O_2 might be attributed to the influence of C_{12}-LAS on electron transfer process occurs from Co^{II}Pc-MWCNTs to Co^{III}Pc-MWCNTs.

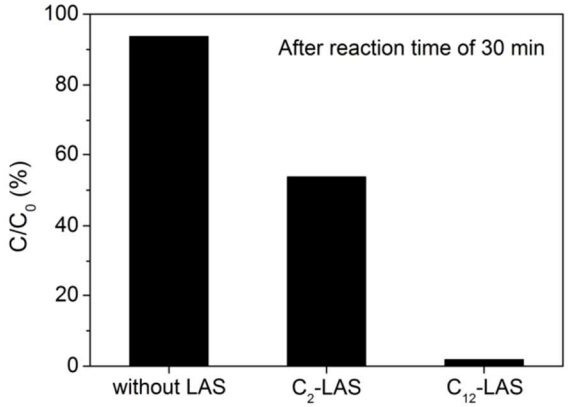

Fig. 6. Catalytic oxidation of AR1 (5×10^{-5} M) by CoPc-MWCNTs activating H_2O_2 (0.01 M) with or without LAS. ([CoPc-MWCNTs]=0.2 g/L (containing 8.88×10^{-6} M of CoPc), [LAS]=5×10^{-3} M , pH 7.55, 50 °C.)

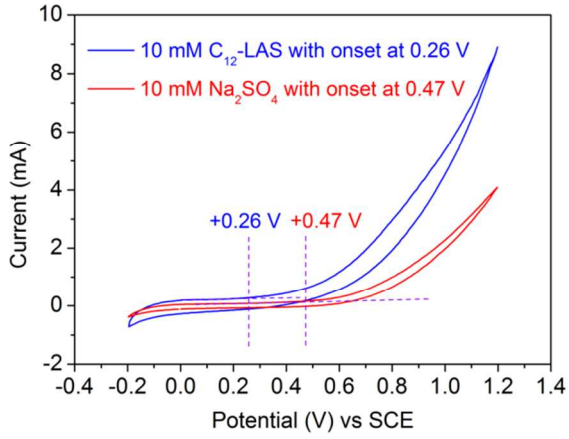

Fig. 7. Cyclic voltammograms of CoPc-MWCNTs with H_2O_2 (0.01 M) in aqueous solution of 0.01 M C_{12}-LAS (blue) and 0.01 M Na_2SO_4 (red) at pH 7.55.

Moreover, the catalytic activity of CoPc-MWCNTs increased with the increasing C_{12}-LAS concentration (Fig. 8), however, such activity dramatically declined when the C_{12}-LAS concentration increased to 20 mM. As shown in the inset image of Fig. 8, after the aqueous solutions of CoPc-MWCNTs with different concentrations of C_{12}-LAS stand for 10 days, the obvious precipitation of catalysts

has been observed in the solution without C_{12}-LAS or with 20 mM C_{12}-LAS. Thus, the reduced activity with 20 mM C_{12}-LAS might be due to the fact that part of CoPc-MWCNTs is tightly wrapped around by the coil of C_{12}-LAS, resulting in substrates and H_2O_2 are difficult to approach the catalytic active sites. Consequently, we can confirm that the SO_3^- group of aryl sulphonates in LAS plays a vitally important role in changing the reaction channel of H_2O_2 activation catalyzed by such supported CoPc, and the linear long-chain structure of C_{12}-LAS has contributed to improve the dispersion of CoPc-MWCNTs.

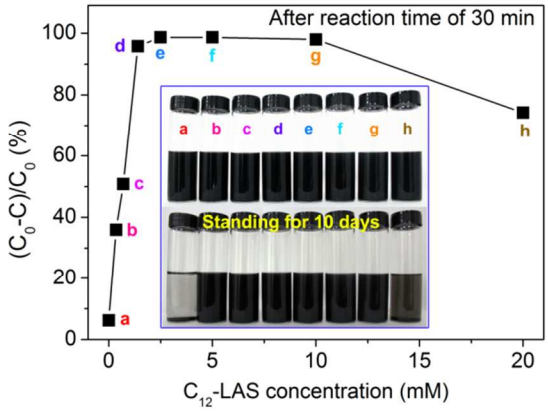

Fig. 8. Effect of C_{12}-LAS concentration on the catalytic oxidation of AR1 (5×10^{-5} M) ([CoPc-MWCNTs]=0.2 g/L, pH 7.55, 50 °C). Inset: Image of the solution of CoPc-MWCNTs with different concentration of C_{12}-LAS after standing for 10 days.

In order to investigate peroxidase-like activity of CoPc-MWCNTs in the presence of C_{12}-LAS, the catalytic oxidation of AR1 has been carried out at different AR1 and H_2O_2 concentrations respectively. The results of Fig. 9 suggest the catalytic system with CoPc-MWCNTs and C_{12}-LAS exhibits a character of enzymatic reaction during the activation of H_2O_2. According to the Michaelis–Menten mode, the main kinetic constants, V_{max} and K_{cat} (Table 1) were 0.572 μM/s and 0.064 s^{-1}. Additionally, although the higher concentration of H_2O_2 maintained the better catalytic activity (Fig. S8), AR1 could be compeletly oxidized with lower concentration of H_2O_2 as long as the reaction time is enough. The improved utilization of H_2O_2 suggests that the reaction channel of H_2O_2 activation catlyzed by CoPc-MWCNTs in the presence of C_{12}-LAS ocurred towards the peroxidase-like process, and the disproportionation of H_2O_2 has been significantly minimized.

3.3 Analysis of the catalytic mechanism

According to the above results, the introduction of LAS dramatically enhanced the catalytic activity of CoPc-MWCNTs for H_2O_2 activation towards the peroxidase-like process. And the non-•OH/•OOH mechanism has been evidenced by results of EPR experiments (Fig. S9), indicating the heterolytic cleavage of the peroxide O-O bond.[8,10,29] Together with the results from Fig. 7, the SO_3^- group of aryl sulphonates in C_{12}-LAS determines the reaction channel of H_2O_2 activation catalyzed by CoPc-MWCNTs. As the enzyme mimic catalyst, CoPc has very analogies in structure and physicochemical properties with metalloporphyrins,[30] which leaves two axial coordination sites on central cobalt ion. During the activation of H_2O_2 catalyzed by CoPc-MWCNTs, one of the axial positions of cobalt ion is coordinated by H_2O_2, and the other axial position is occupied by C_{12}-LAS. It has been recognized that the O atom from SO_3^- group of aryl sulphonates could coordinate with the divalent transition metal atoms which lie on an inversion center and are coordinated by four N atoms.[31-34] Similar coordination behavior could occur in system with CoPc-MWCNTs and C_{12}-LAS because of the Co-N_4 macrocycles in CoPc, and the heterolytic cleavage of the peroxide O-O bond might occur accompanying the formation of high valent cobalt-oxo oxidant. Such active intermediates has been characterized in iron phthalocyanine systems for activating H_2O_2 or other peroxides by the heterolytic cleavage of O-O bond without •OH production.[35-37]

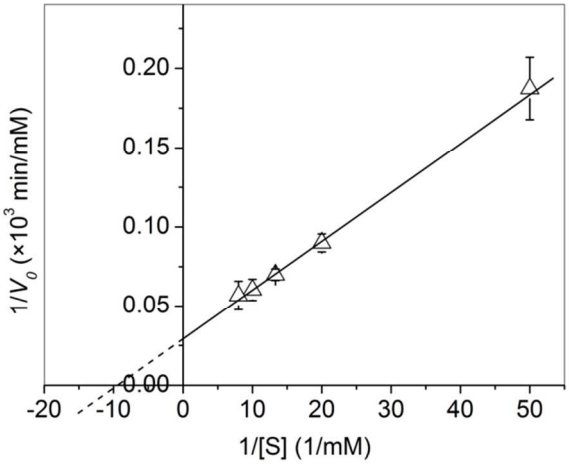

Fig. 9. Lineweaver-Burke plots for the peroxidase activity of CoPc-MWCNTs activating H_2O_2 with AR1 as the substrate.

Table 1. Kinetic Constants of CoPc-MWCNTs activating H_2O_2

K_m (mM)	V_{max} (μM/s)	K_{cat} (s^{-1})	K_{cat}/K_m (s^{-1} mM^{-1})
0.106	0.572	0.064	0.607

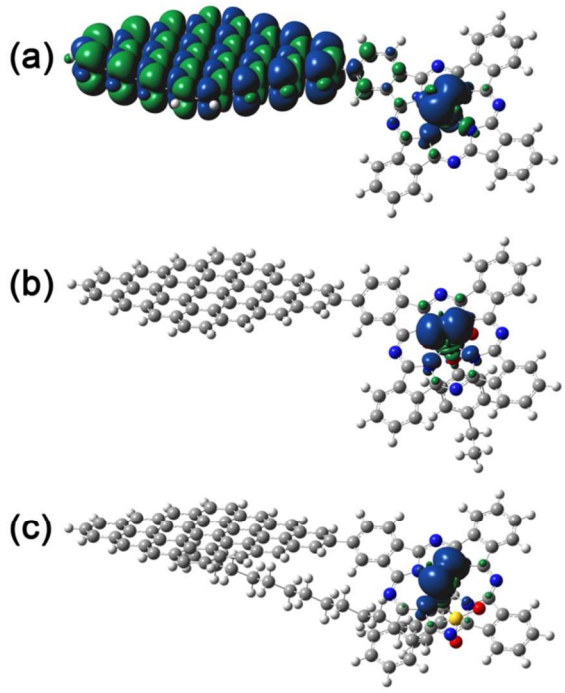

Fig. 10. DFT calculated spin density distributions of the generated intermediates at the B3LYP/6-31G level of theory in the catalytic system of CoPc-MWCNTs for activating H_2O_2 (a) without LAS, with (b) C_2-LAS and (c) C_{12}-LAS, respectively.

Further, according to the results of DFT calculations using graphite as a coronene-like planar sheet to model the CoPc-

MWCNTs (Fig. S10), the calculated spin density distribution is found to be in good agreement with experimental results. The results of the calculated bond distances in Table S1 confirm the formation of Co^{IV}=O, and the bond distance of cobalt-oxo is shorter than Co-O (SO_3^-) of LAS (C_2-LAS and C_{12}-LAS). Without the fifth ligands of LAS, spin delocalization occurs onto MWCNTs and Co ions (Fig. 10a), which agree with our previous results that the active sites on MWCNTs could participate in the oxidation of substrate.[19] With C_2-LAS or C_{12}-LAS, spin delocalization occurs onto the center Co ions (Fig. 10b and Fig. 10c). We can confirm that the high-valent MWCNT-CoPc-oxo intermediates have been formed in the presence of LAS and could afford the powerful active species to oxidize substrates by the peroxidase-like process. These active species are covalently anchored on the surface of MWCNTs, facilitating the enhanced activity by shortening the DMTP. Moreover, the hydrophobic interaction between MWCNTs and the alkyl long-chain of C_{12}-LAS could improve the dispersion of CoPc-MWCNTs, ensuring the catalytic oxidation occur in a good suspension system.

4 Conclusions

We describe a bioinspired catalytic system for H_2O_2 activation based on CoPc-MWCNTs and the fifth ligands. CoPc-MWCNTs were prepared by a one-step deamination reaction under the moderate condition. The reaction channel of H_2O_2 activation catalyzed by CoPc-MWCNTs has been controlled in the presence of LAS, facilitating the peroxidase-like process and improving the utilization of H_2O_2. The generated high-valent cobalt-oxo intermediates are bonded on the surface of MWCNTs, reducing the transfer resistance of substrates. This study attempts to construct an enzyme-mimic system using MWCNTs to support the catalytic entity, and the introduction of the fifth ligands mimic the functions of cofactors in natural enzymes. This work not only successfully develops a source of inspiration to design the catalysts of artificial enzymes for practical applications, also reveals further insight into the approach to improve the overall catalytic performance of traditional catalysts by employing CNTs as supports, realizing the catalytic reactions that were not possible in the past. We expect that CNT-based enzyme-mimic catalysts with unique properties and functions will attract increasing research interest and create new opportunities in various research fields of functional materials.

Acknowledgements

This work was supported by the National Natural Science Foundation of China (No. 51133006, 51302246 and 51103133), Textile Vision Science & Education Fund, 521 Talent Project of ZSTU, and Zhejiang Provincial Natural Science Foundation of China (No. LY14E030013 and LY14E030015).

Notes and references

[a] National Engineering Lab for Textile Fiber Materials & Processing Technology (Zhejiang), Zhejiang Sci-Tech University, Hangzhou 310018, China. E-mail:luwy@zstu.edu.cn(W. Lu); wxchen@zstu.edu.cn(W. Chen)

[b] Department of Chemistry, Zhejiang Sci-Tech University, Hangzhou 310018, China.

† Electronic Supplementary Information (ESI) available: The XPS Co1s data, UV-vis spectra, raman spectra, dynamic thermogravinmetric analytical results, the EPR spectra, the calculated bond lengths for the energy minimized DFT models and the catalytic performance of CoPc-MWCNTs under other different conditions. See DOI: 10.1039/b000000x/

1 R. Hage and A. Lienke, *Angew. Chem., Int. Ed.*, 2006, **45**, 206.
2 C. Wang and H. Yamamoto, *J. Am. Chem. Soc.*, 2014, **136**, 1222.
3 G. Fang, J. Gao, C. Liu, D. D. Dionysiou, Y. Wang and D. Zhou, *Environ. Sci. Technol.*, 2014, **48**, 1902.
4 T. Hwang, B. R. Goldsmith, B. Peters and S. L. Scott, *Inorg. Chem.*, 2013, **52**, 13904.
5 Y. Wang, D. Janardanan, D. Usharani, K. Han, L. Que, Jr. and S. Shaik, *ACS Catal.*, 2013, **3**, 1334.
6 N. J. Schoenfeldt, Z. Ni, A. W. Korinda, R. J. Meyer and J. M. Notestein, *J. Am. Chem. Soc.*, 2011, **133**, 18684.
7 P. Borah, X. Ma, K. T. Nguyen and Y. Zhao, *Angew. Chem., Int. Ed.*, 2012, **51**, 7756.
8 T. J. Collins, *Acc. Chem. Res.*, 2002, **35**, 782.
9 M. Ghosh, K. K. Singh, C. Panda, A. Weitz, M. P. Hendrich, T. J. Collins, B. B. Dhar and S. S. Gupta, *J. Am. Chem. Soc.*, 2014, **136**, 9524.
10 L. Que and W. B. Tolman, *Nature*, 2008, **455**, 333.
11 J. H. Dawson, *Science*, 1988, **240**, 433.
12 G. I. Berglund, G. H. Carlsson, A. T. Smith, H. Szöke, A. Henriksen and J. Hajdu, *Nature*, 2002, **417**, 463.
13 T. J. Reid, M. R. Murthy, A. Sicignano, N. Tanaka, W. D. Musick and M. G. Rossmann, *Proc. Natl. Acad. Sci. U.S.A.*, 1981, **78**, 4767.
14 N. Li, W. Lu, K. Pei, Y. Yao and W. Chen, *Appl. Catal., B*, 2015, **163**, 105.
15 H. Wang, S. Li, Y. Si, N. Zhang, Z. Sun, H. Wu and Y. Lin, *Nanoscale*, 2014, **6**, 8107.
16 K. Elouarzaki, A. Le Goff, M. Holzinger, C. Agnès, F. Duclairoir, J. Putaux and S. Cosnier, *Nanoscale*, 2014, **6**, 8556.
17 X. Gu, W. Qi, X. Xu, Z. Sun, L. Zhang, W. Liu, X. Pan and D. Su, *Nanoscale*, 2014, **6**, 6609.
18 W. Lu, N. Li, W. Chen and Y. Yao, *Carbon*, 2009, **47**, 3337.
19 W. Lu, N. Li, S. Bao, W. Chen and Y. Yao, *Carbon*, 2011, **49**, 1699.
20 A. Ghosh, D. A. Mitchell, A. Chanda, A. D. Ryabov, D. L. Popescu, E. C. Upham, G. J. Collins and T. J. Collins, *J. Am. Chem. Soc.*, 2008, **130**, 15116.
21 Z. Li, W. Yan and S. Dai, *Langmuir*, 2005, **21**, 11999.
22 J. P. Dodelet, Oxygen Reduction in PEM Fuel Cell Conditions: Heat-treated Non-precious Metal-N4 Macrocycles and Beyond. J. H. Zagal, F. Bedioui, J. P. Dodelet, Eds.; Springer New York, 2006; Chapter 3, 83-147.
23 J. C. Swarbrick,; T. C. Weng, K. Schulte, A. N. Khlobystov and P. Glatzel, *Phys. Chem. Chem. Phys.*, 2010, **12**, 9693.
24 Y. K. Kang, O. S. Lee, P. Deria, S. H. Kim, T. H. Park, D. A. Bonnell, J. G. Saven and M. J. Therien, *Nano Lett.*, 2009, **9**, 1414.
25 M. Quintana, H. Traboulsi, A. Llanes-Pallas, R. Marega, D. Bonifazi and M. Prato, *ACS Nano*, 2012, **6**, 23.
26 J. Park, P. Deria and M. J. Therien, *J. Am. Chem. Soc.*, 2011, **133**, 17156.
27 P. N. Mashazi, K. I. Ozoemena and T. Nyokong, *Electrochim. Acta*, 2006, **52**, 177.
28 T. Kondo, A. Tamura and T. Kawai, *J. Electrochem. Soc.*, 2009, **156**, 145.
29 D. P. Goldberg, *Acc. Chem. Res.*, 2007, **40**, 626.
30 A. B. Sorokin, *Chem. Rev.*, 2013, **113**, 8152.

31 K. Zhang, X. Meng and X. Li, *Acta Crystallogr., Sect. E: Struct. Rep. Online*, 2009, **E65**, m1678.
32 I. Murase, G. Vuckovic, M. Kodera, H. Harada, N. Matsumoto, and S. Kida, *Inorg. Chem.*, 1991, **30**, 728.
33 M. R. Sundberg and R. Sillanpääb, *Acta Chem. Scand.*, 1993, **47**, 1173.
34 T. M. Cocker and R. E. Bachman, *Chem. Commun.*, 1999, 875.
35 P. Afanasiev, E. V. Kudrik, F. Albrieux, V. Briois, O. I. Koifman and A. B. Sorokin, *Chem. Commun.*, 2012, **48**, 6088.
36 P. Afanasiev, E. V. Kudrik, J. J. M. Millet, D. Bouchu and A. B. Sorokin, *Dalton Trans.*, 2011, **40**, 701.
37 A. B. Sorokin, E. V. Kudrik, L. X. Alvarez, P. Afanasiev, J. M. M. Millet and D. Bouchu, *Catal. Today*, 2010, **157**, 149.